RAS Techniques and Instruments

RASTAI **3,** 705–710 (2024) https://doi.org/10.1093/rasti/rzae044
Advance Access publication 2024 November 4

Noise test of an electromagnetic antenna for low frequency scattered gravitational waves

Adrian Michael Cruise[1,2]★ and Robert Flack[1]

[1]*Department of Physics and Astronomy, University College London, Gower Street, London, WC1E 6BT, UK*
[2]*School of Physics and Astronomy, University of Birmingham, Edgbaston, Birmingham, B15 2TT, UK*

Accepted 2024 October 21. Received 2024 August 16; in original form 2024 February 1

ABSTRACT

Gravitational waves proved hard to detect experimentally and yet carry high energy fluxes. Conversely, the technology for electromagnetic waves is sophisticated, easily available, and highly sensitive. Various proposals have been made to use the conversion of a gravitational wave into an electromagnetic wave to generate signals that could be detected. We present test results from a novel electromagnetic antenna, efficient at the very low frequencies needed to explore the signals from supermassive black holes mergers. These will eventually be studied by the *laser interferometric space antenna* (*LISA*) at wavelengths between 10^8 and 10^{11} m. Common forms of electromagnetic antennae are only efficient when the ratio of wavelength, λ, to antenna length, L, is roughly between 0.1 and 10. This paper proposes a scheme for a realistic ground-based electromagnetic antenna, 'the resistive antenna', which operates efficiently at a ratio $\frac{\lambda}{L}$ of more than 10^6. The first estimates of ambient noise at these low frequencies from field trials of such a device are presented. The measured levels of ambient noise result in this detection scheme having a sensitivity much worse than *LISA*. The antenna design described in this communication may also have application in other fields.

Key words: Instrumentation – Gravitational Waves – Electromagnetic Antenna.

1 INTRODUCTION

The scientific motivation to expand gravitational wave astronomy is very strong. Results from the laser interferometric gravitational observatory (*LIGO*) (Abbott & et al. 2016) are helping to build a picture of the population and evolution of stellar-sized black holes and the laser interferometry employed by *LIGO* is actively being made ready for use in a space based detector, *laser interferometric space antenna* (*LISA)* (Vitale 2014), aimed at studying massive black holes and their influence on galaxy formation. With the launch date for *LISA* more than a decade away, alternative detection strategies might be of interest even if they are less effective than the current *LISA* design. Detection of gravitational waves at mHz frequencies pose a range of new technical challenges. The physical effect of the gravitational to electromagnetic conversion process is an electromagnetic wave at the same frequency as the incoming gravitational wave. For gravitational waves at frequencies of about 1 mHz this implies the detection system must be efficient in transforming electromagnetic waves with a wavelength of 3×10^{11} m into an electrical signal using structures (the antenna) smaller by a factor of the order of 10^9. This requires an unusual design of electromagnetic antenna, and a design for a ground-based antenna meeting this requirement is presented in this communication, together with results of field trials investigating the ambient electromagnetic noise at these frequencies.

2 GW TO EMW CONVERSION

The interaction of gravitational waves and electromagnetic fields has been studied from many aspects and a considerable literature has built up over the years. The first relevant calculations were performed by Gertsenshtein (1962) for the case of the conversion from electromagnetic to gravitational waves in a static magnetic field and these were extended by Lupanov (1967) to the case of a static electric field. One of the easiest geometries to understand is the interaction of a plane gravitational wave with a magnetized body, in particular a magnetized sphere. Viewing such an interaction as a scattering process leads to the normal separation into two regimes depending on whether the wavelength, λ, of the gravitational wave is larger or smaller than the radius, R, of the scattering sphere. The Gershenstein study examined the case in which $\lambda \ll R$ and showed that the power flux conversion increased as $\left(\frac{\lambda}{R}\right)^2$ provided the phase velocity of the gravitational and electromagnetic waves were equal throughout the interaction volume. For laboratory detectors with magnet dimensions of the order of metres or less, the wavelength restriction $\lambda \ll R$ implies frequencies higher than 300 MHz – a part of the spectrum not expected to be illuminated by strong gravitational waves from known astronomical bodies, although the potential for sources and detection at these very high frequencies has been explored in previous publications (Cruise 2012; Aggarwal et al. 2021).

The second scattering regime is one in which $\lambda \gg R$ and the magnetized sphere appears as a point scatterer. With astronomical sources of gravitational waves predicted at frequencies in the range 1 kHz

★ E-mail: m.cruise@ucl.ac.uk

$(\lambda = 3 \times 10^5\,\mathrm{m})$ to 0.1 mHz $(\lambda = 3 \times 10^{12}\,\mathrm{m})$) even planets and stars can satisfy this wavelength constraint for parts of the spectrum. The point scatterer case has been studied by De Logi & Mickelson (1977) and by Boccaletti et al. (1970) using very different theoretical approaches. De Logi and Mickleson calculated the scattering cross-section for conversion from gravitons to photons in the external field of a magnetized sphere using the Feynman formalism. The scattering efficiency calculation results in a relationship between the incoming gravitational wave energy flux F_{gw} and the outgoing electromagnetic energy flux F_{emw} scattered at frequency ω from an object with magnetic moment M, in geometrized units (G=c=$\hbar$=1), omitting angular factors, of the form:

$$F_{\mathrm{emw}} \sim \sigma \omega^2 M^2 F_{\mathrm{gw}}. \tag{1}$$

Not unexpectedly, the value for the scattering cross-section, σ, is small. For the energy fluxes in Wm^{-2}, the frequency in Hz and the magnetic moment in JT^{-1} or Am^2, σ has the value 8.1×10^{-69} for the case studied. This arises basically from the very small 'graviton–photon' vertex factor $\frac{\mathrm{G}}{\mathrm{c}^2}$, although the Feynman formalism is not restricted to quantized fields. However, as pointed out in the introduction, gravitational waves of the expected dimensionless amplitude h (with $h \sim 10^{-22}$, say) represent a considerable energy flux (Maggiore 2008) of $F_{\mathrm{gw}} = \frac{1}{32\pi}\frac{\mathrm{c}^3}{\mathrm{G}}\omega^2 h^2$ so that many factors of G and c in the product σF_{gw} cancel, giving rise to electromagnetic fluxes which may not be beyond detection. V De Sabbata & Gualdi (1974) used a classical field theory approach to calculating the electromagnetic energy flux resulting from the scattering from the magnetized sphere itself (neglecting the external dipole field) and obtained a similar expression to that of De Logi and Mickelson, apart from some angular factors, but with a significantly larger value for σ of 1.8×10^{-64}.

3 POTENTIAL SCATTERERS

Normal laboratory experiments can access strong magnetic fields with several different technologies. Rare Earth magnets can provide surface fields approaching 1 T for magnets of centimetre size giving a magnetic moment of the order of $\sim 10^{-5}\,\mathrm{JT}^{-1}$ while superconducting magnets can provide up to 40 T over a volume of the order of $1 \times \mathrm{m}^3$ giving a magnetic moment of the order of $\sim 10^2\,\mathrm{JT}^{-1}$. It is possible to form a rough estimate of the magnetic moment of planets and stars by measuring their radius, R, and the surface field, B. In SI units the magnetic moment in JT^{-1} can be approximated as $M \sim BR^3$. In the case of the Sun, estimates of $3 \times 10^{30}\,\mathrm{JT}^{-1}$ for the dipole moment have been published, for Jupiter $M = 6.3 \times 10^{27}\,\mathrm{JT}^{-1}$ and for the Earth extensive geomagnetic studies give a measured value of $M = 7.95 \times 10^{22}\,\mathrm{JT}^{-1}$ (Durand-Manterola 2009). These large values for the magnetic dipole moment of local astronomical bodies indicate that gravitational waves are being converted into electromagnetic waves in the Solar System with an efficiency which is worthy of investigation, even at frequencies low enough to come from credible sources. However, generating the electromagnetic waves is not enough to provide a useful detection strategy. The electromagnetic waves must propagate from the scattering body, be collected by an efficient antenna connected to the detector, and be detectable against likely noise sources. A fundamental noise limit in any detector is set by internal noise be it thermal or a quantum noise process in origin. In trying to detect the converted electromagnetic waves using detectors in various Solar System geometries, the signals also have to be differentiated from local environmental noise which may be far greater than the internal noise of the detector. To measure such local environmental noise an antenna effective at these extreme values of $\frac{\lambda}{L}$ is required.

This communication describes such a scheme for detecting the low frequencies emitted by sources in the *LISA* band, together with preliminary estimates of ambient electromagnetic noise levels.

4 COMMON ANTENNA TYPES AND THEIR PERFORMANCE

Antenna theory is a well developed branch of electrical engineering and the properties of the common forms of antenna are well known (Kraus & Marhefka 2003). Antennae for normal communications operate in a regime in which the ratio of wavelength to antenna length, $\frac{\lambda}{L}$, lies between 0.1 and 10. There are exceptions when specific antenna properties are required but in general the performance of common antenna designs falls off rapidly as $\frac{\lambda}{L}$ increases beyond 10.

An antenna has an 'effective area', A_{eff} in m^2, which can be used to characterize how much energy is extracted from an electromagnetic wave having a power flux P expressed in Wm^{-2} such that the power received, $P_{\mathrm{rec}} = A_{\mathrm{eff}} P$. The effective area of an antenna is usually calculated using the theory of reciprocity (Kraus & Marhefka 2003) which states that the receiving properties of an antenna are the same as its transmitting properties. By postulating an oscillating current at a certain frequency, ω, flowing in the antenna structure when transmitting, the magnitudes of the electric and magnetic fields, E and B, can be computed and the Poynting vector at a distant point calculated. This relationship between an oscillating current and the distant power flow can then be reversed using the theory of reciprocity to calculate the induced current derived from a certain ambient power flux when the antenna is used for reception. Since the induced current is related to the ambient power flux by a quantity having the dimensions of resistance, antenna designers calculate a 'radiation resistance' to express this relationship.

For an antenna having radiation resistance, R_{rad}, Ohmic losses, R_{loss} in the conductor, and a residual complex impedance, X, the effective area is given by:

$$A_{\mathrm{eff}} = G\frac{\lambda^2}{4\pi}\left(\frac{R_{\mathrm{rad}}}{R_{\mathrm{rad}} + R_{\mathrm{loss}} + X}\right), \tag{2}$$

where G is the gain of the antenna, essentially the inverse of its angular area of reception or transmission. For an isolated antenna small in comparison to the wavelength of operation, G is usually about 1.5. The antenna performance can be maximized by 'tuning' the system in such a way as to reduce X to zero by the addition of either inductive or capacitative reactance of opposite sign to that of the untuned antenna. Such tuning is only effective at one frequency and therefore unsuitable for wideband reception. In this case, another suboptimal feature which reduces the effective area is the presence of Ohmic losses which are usually minimized by using good conductors with low resistance.

With these properties of antennae defined, different antenna geometries can be assessed for use at low frequencies.

The simple dipole antenna formed from conductors of diameter a, has a radiation resistance given by Kraus & Marhefka (2003):

$$R_{\mathrm{rad}} = 80\pi^2\left(\frac{L}{\lambda}\right)^2\,\Omega. \tag{3}$$

While this expression leads to a constant value for the effective area as the wavelength varies, unfortunately the antenna reactance has the form:

$$X = -\frac{120\lambda}{\pi L}\left(ln\left(\frac{L}{2a}\right) - 1\right). \tag{4}$$

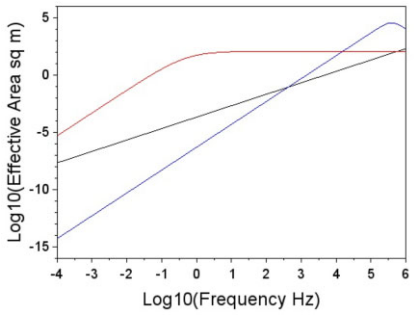

Figure 1. Effective area of several generic forms of antenna versus frequency. Dipole (middle curve at lowest frequency), Loop (lowest curve at lowest frequency), 'Resistive Antenna' (upper curve at lowest frequency). All formats are assumed to have a linear size of 100 m a conductor diameter of 1mm and an ohmic resistance of 0.021 $\Omega\,m^{-1}$. The resistive antenna parameters were $R1$=15Ω and $R2$=65Ω. The Earth capacitance was assumed to be 700 μF.

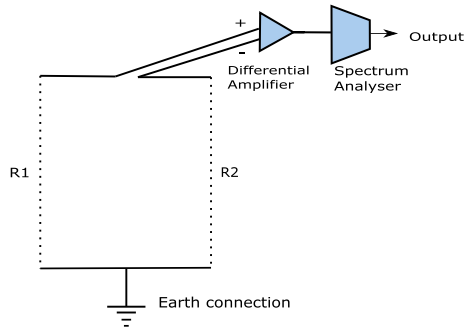

Figure 2. A schematic diagram of the resistive loop antenna described in the text. $R1$ and $R2$ are the sections of the loop made from constantan resistance wire.

At the low frequencies being considered here this reactance term can be of the order of 10^{12} Ohms, much too large to be 'tuned out' by practical reactive components and therefore substantially diminishing the effective area and antenna performance.

An antenna geometry which avoids this problem of untuned reactance is the loop antenna. This is a square or circular conducting loop with a small gap across which the voltage generated can be measured. The radiation resistance of a loop antenna of geometric area, A, is given by:

$$R_{\rm rad} = 31\,200\left(\frac{A}{\lambda^2}\right)^2 \text{ Ohm}. \tag{5}$$

Inserting this expression into equation(2) gives an effective area that reduces as the square of the wavelength, again offering poor performance in the frequency range of interest.

Fig. 1 shows the effective area of the loop antenna (lowest curve at low frequency) and the dipole antenna (middle curve at low frequency) as a function of frequency over the range of current interest to gravitational wave astronomy. In each case the antenna is assumed to have a linear size of 100 m. The effective area of a third antenna, also 100 m in size, of a radically different design is also plotted as the highest curve at low frequency. This is described in the next section under the title 'Resistive Antenna' and is developed here specifically to provide high efficiencies at low frequencies.

5 THE RESISTIVE ANTENNA

A conductor of length, L, immersed in an electric field, E, parallel to its length can experience a current flowing in it and therefore a voltage developed along it provided there is a suitable sink for the current. The magnitude of the current induced depends on the internal impedance (in this case the impedance of free space, 377 Ω) of the source of the electric field, $R_{\rm int}$, the resistance of the conductor, $R_{\rm cond}$, and in the case that the wavelength is longer than the antenna, the resistance between the conductor and the necessary sink for the current, $R_{\rm sink}$. If the wavelength of the electromagnetic wave generating the electric field is much smaller than the size of the antenna then currents localized on the scale of a wavelength can generate voltages with no nett current flow to a sink of charge. Resistive sheets known as Salisbury cloth Kraus & Fleisch (1999) are used to absorb microwave radiation in exactly this mode of operation.

It is assumed that $R_{\rm int}$ is the impedance of free space with a value of 377 Ω for an electromagnetic wave travelling in vacuum.

The voltage generated in a single resistive conductor with the properties defined above will be:

$$V = E.L\left(\frac{R_{\rm cond}}{R_{\rm cond} + R_{\rm int} + R_{\rm sink}}\right). \tag{6}$$

In order to make a practical antenna from such a principle the voltage generated across the conductor has to be delivered to a suitable low noise amplifier by means of two shielded cables, one attached to each end of the conductor. A substantial performance advantage can be achieved from the common mode rejection properties of differential amplifiers if the two signal cables follow essentially identical paths and therefore pick up identical spurious signals which cancel out in the differential amplifier. This requires that the two output terminals of the antenna should be extremely close together, not separated by the antenna scale, L. One way of achieving this is to place two parallel resistive conductors in the electric field with different resistances, joined at the remote end by a connection to a current sink such as the Earth. If the resistance of the two conductors, $R1$ and $R2$, are different then even though only the difference in the two generated voltages is measured, a non-zero voltage results. A schematic diagram of such a system is shown in Fig 2. In this configuration the voltage generated is given by:

$$V = E.L.abs\left(\left(\frac{R1}{R1 + R_{\rm int} + R_{\rm sink}}\right) - \left(\frac{R2}{R2 + R_{\rm int} + R_{\rm sink}}\right)\right) \tag{7}$$

To simplify the remaining text a function $f\,(R1, R2, R_{\rm sink})$ can be defined as:

$$f\,(R1, R2, R_{\rm sink}) = abs\left(\left(\frac{R1}{R1 + R_{\rm int} + R_{\rm sink}}\right) - \left(\frac{R2}{R2 + R_{\rm int} + R_{\rm sink}}\right)\right). \tag{8}$$

Following this analysis the effective area of an antenna constructed along these lines is $A_{\rm eff} = L^2 f^2\,(R1, R2, R_{\rm sink})$ and it is this quantity which is the upper curve at low frequencies in Fig. 1.

6 THE CURRENT SINK

Crucial to the operation of this resistive antenna is the requirement for a current flow through the conductors. The natural choice, in the case of a terrestrial detector, is to connect the two resistive conductors to the Earth or ground via as low a resistance path as possible. This can act as an efficient current sink provided the voltage of the ground

connection does not materially change as the charge is delivered, this is a property of a high electrostatic capacity. The Earth does not have infinite capacitance but a value of 700 μF can be calculated from its radius. In the calculations underlying Fig. 1, the value of $R_{\rm sink}$ is the sum of whatever Ohmic resistance there may be in the ground connection and the impedance at the instrument frequency of the Earth capacity, C, hence:

$$R_{\rm sink} = R_{\rm ground} + \left(\frac{1}{2\pi\omega C}\right). \quad (9)$$

As the frequency reduces, this last term dominates the sensitivity of the antenna which falls off below 10^{-2} Hz, although it remains many orders of magnitude above that of dipoles and loop antennae across the $LISA$ frequency range.

7 SIMULATIONS

The validity of the analysis presented for the resistive antenna has been tested using the Finite Difference Time Domain (FDTD) electromagnetic field solver code (Taflove & Hagness 2005). The limitations of memory size constrain the wavelength range of the simulations to values of $\left(\frac{\lambda}{L}\right) < 20$, far from the wavelength regime for which the antenna is designed. However the signals generated in these simulations followed the predicted values for a range of ($R1$, $R2$) pairs to a good accuracy.

8 FIELD TRIALS AT $\frac{\lambda}{L} \sim 1500$

To completely validate the performance of the resistive antenna a source of plane electromagnetic waves at the intended frequency of operation, 1–10 mHz, would be needed representing a value for $\left(\frac{\lambda}{L}\right)$ of the order of 10^{11}. No such source of radiation is known to the authors but the closest local approximation was the BBC Long Wave transmitter at Droitwich Pawley (1972) which radiates at 198 kHz (a wavelength of approximately 1500 m). This signal source had the advantage that there was only one transmitting antenna within 1000 km with significant emitted power on this frequency and it was 120 km from the test receiving antenna. At this distance of 80 wavelengths the radiation field should approximate a plane wave except for small ground distortions. These measurements were made in 2017, the Droitwich transmitter ceased operation in 2023.

To test this antenna design a square antenna having sides 1 m long was constructed with the two vertical sections constructed from constantan resistance wire of different resistivities. This geometry was suitable for signals with the electric field in a vertical position. The lower horizontal section was low resistance copper wire connected at its midpoint to earth. The upper horizontal section was split at its midpoint to provide two terminals for the voltage measurement via shielded cables to a Stanford SR560 differential amplifier with a common mode rejection ratio of 40 db. (Shielding of the cables reduces any mutual inductance to extremely low levels and reduces pickup from external sources.) The output of the amplifier was connected to an AOR 5000 communications receiver tuned to 198 kHz with an AOR 5600 spectrum analyser connected to the IF output. The spectrum analyser provided a means of making power measurements of the 198 kHz signal to an accuracy of 1 dbm without confusion from other nearby signals. The complete measurement system including cables was calibrated by connecting a 198 kHz signal of measured amplitude to the antenna cables via calibrated attenuators and recording the spectrum analyser power level. The data from this process was used to determine a relationship between the measured power and the input signal amplitude. A schematic diagram of the loop antenna is presented in Fig. 2.

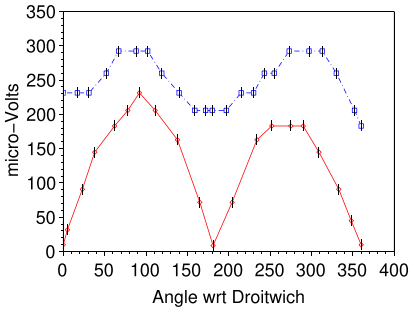

Figure 3. Signal voltage from square resistive loop antenna operated in two modes. Upper data are output from antenna in normal loop mode as a function of angle to source. Lower data are from loop earthed at midpoint to current sink.

The antenna had the geometric format of a normal square loop antenna when the ground connection was absent, albeit a loop with considerable Ohmic losses due to the resistance wire elements. This mode of performance as a simple loop antenna was confirmed by rotating the square loop about a vertical axis so that the normal to the plane made an azimuthal scan. The results were in agreement with the expected output from a loop antenna with a strong null when the normal to the plane of the loop was directed towards the signal source as shown in the lower curve in Fig. 3. The peak signal voltage received can be used to determine the ambient electromagnetic field generated by the Droitwich transmitter at the antenna by using equations (6) and (7). The Ohmic loss resistance of the loop, $R_{\rm loss}$, was 78.68 Ω and the reactive impedance, X, was 6.09 Ω.

The lower data points in Fig. 3 were recorded by changing the antenna to its 'resistive mode' simply by connecting the midpoint of the lower horizontal section to Earth, thereby providing the current sink described in Section6.

In this mode the predictions from equation (7) for the signal expected using a range of different ($R1$, $R2$) resistance pairs can be compared to the power measured by the 198 kHz receiver described above. A series of 14 values for the ($R1$, $R2$) pairs was used to explore the antenna performance. Due account was taken in the analysis of the capacitance to earth of the cables running from the resistive antenna to the differential amplifier. This capacitance was measured as 2001 pF and acted as a shunt impedance to each of $R1$ and $R2$. The length, L, of the sides of the loop was known as were the values of $R1$ and $R2$ for each data point. The two unknowns for this data set were E, the ambient electric field amplitude at 198 kHz and $R_{\rm sink}$ the resistance in the path to the current sink. At the frequency of operation, $f = 198$ kHz, the value of $R_{\rm sink}$ is completely dominated by ohmic resistance in the ground connection and the effect of the finite capacity of the earth only contributes of the order of 10^{-3} Ω. A chi-squared fit of the data points to equation (7) determined the best fitted values of E and $R_{\rm sink}$. Fig. 4 shows the measured dependence of the detected power on the f-factor of the antenna for the best-fitting values. The chi-squared was 7.9 for 11 degrees of freedom, indicating a good fit. As an independent test of this procedure, the best-fitting value for $E = 1.93 \times 10^{-4}$ Vm^{-1} was in fairly good agreement with the measurement of the ambient 198 kHz electric field, 2.51×10^{-4} Vm^{-1}, obtained using the antenna in its loop mode.

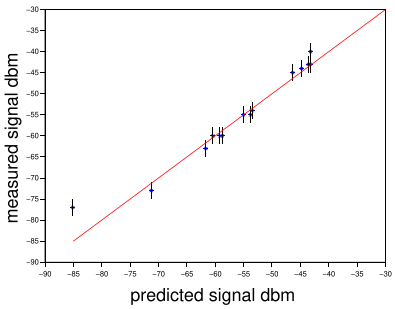

Figure 4. Signal power from distant source provided by 1 m x 1 m square loop with different resistivity arms versus theoretical predictions from equation (7).

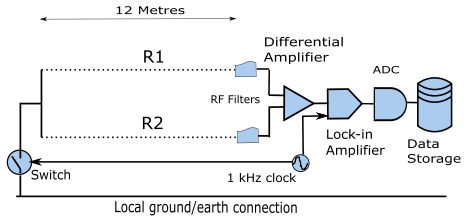

Figure 5. The signal processing chain from the two resistive arms of the antenna through to the data storage system.

9 AMBIENT ENVIRONMENTAL NOISE IN THE MHZ RANGE

To test this scheme for very low frequency ambient noise, a resistive antenna was constructed of two, parallel, horizontal wires of constantan separated vertically by approximately 1 m. The schematic diagram of the antenna and the analogue processing electronics is shown in Fig.5, in a geometry suitable for the reception of signals with the E-Field horizontal. The lower wire being about 1m above ground level. At one end, the wires were connected together and, via an analogue switch running at 1 kHz, also connected to earth. At the other end, the two wires were connected to the input of a differential amplifier feeding a 1kHz lock-in amplifier synchronized by the 1 kHz signal from the clock that drove the analogue switch. The use of a lock-in amplifier working at 1kHz effectively heterodyned the signals away from the low frequency properties of the resistive antenna illustrated in Fig. 1 since the reactance of the Earth's capacitance at 1 kHz is negligible. So $R_{\rm sink}$ is equal to $R_{\rm ground}$ to high precision in equation (9). The lock-in amplifier inputs were heavily filtered (in excess of 100 db) at RF frequencies to prevent breakthrough from radio broadcast stations. The gain of the amplifiers was 16 804 and these fed a Picolog AD24 ADC under control of a laptop PC. The ADC had 24 bit resolution and sampled at 1 Hz. The intrinsic noise level of the system was measured by recording data sets of length 5000 s with the input to the differential amplifier shorted. Data were also taken in the field trials with the resistive antenna replaced by a shielded aluminium box containing passive electronic components, resistors, which matched in value the resistance of the resistive antenna. This 'false antenna' data provided a check on any change in the intrinsic noise properties of the system between the bench tests and the field environment and was broadly consistent with the intrinsic system noise. All data sets were 5000 s long and had variations due to temperature removed in the analysis. A fourth order polynomial was fitted to remove other forms of drift

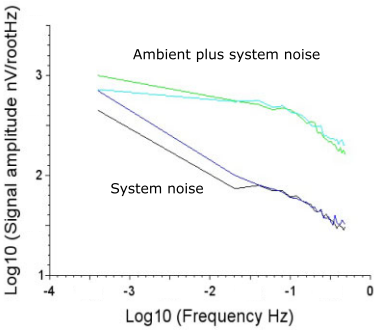

Figure 6. Ambient noise spectra for 12 m resistive antenna (upper curves) compared to system noise measurements (lower curves).

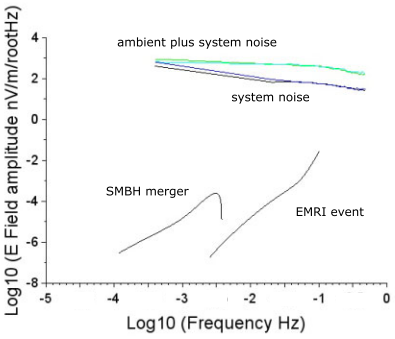

Figure 7. Ambient noise spectra for a 12 m resistive antenna (upper curves) compared to predictions of signals from SMBH merger ($h\sim 10^{-17}$) and an EMRI event ($h\sim 10^{-18}$).

and Fourier spectra were calculated with a frequency resolution of 400 μHz. The spectra displayed here are the result of averaging over 100 channels to improve the statistical quality. The data from the ambient noise measurements, Fig. 6, show a significant excess of electromagnetic noise between 1 mHz and 0.5 Hz of several hundred picoV per root Hz. Ambient electrical noise at this level would set a limit on the gravitational wave sensitivity available from a resistive antenna of this size using the conversion of gravitational waves to electromagnetic waves in the Earth's magnetic field, unless its source could be identified and systematically removed.

10 IMPLICATIONS FOR GW SENSITIVITY

Estimates of the electromagnetic signal provided by such an antenna system in response to well modelled gravitational wave sources such as supermassive black hole (SMBH) mergers and extreme mass ratio inspirals (EMRI) events are illustrated in Fig. 7. The spectrum of electromagnetic radiation from these events is significantly distorted by the ω^2 factor in the scattering equation but, for the frequency range under study, all the signals fall in the point scattering regime with a higher value of σ. The data plotted in Fig. 7 are in electric field units of nVm^{-1}, so in principle the astronomical signals might be enhanced by using a longer resistive antennae, say up to a km in length to overcome the system noise. However, without identifying the source of the ambient electromagnetic noise it is not known whether this source of electromagnetic signal is also proportional to antenna length. The amplitude predictions for the SMBH merger (with a maximum dimensional amplitude of 10^{-17}) and the EMRI event (with a maximum dimensional amplitude of

10^{-18}) were made assuming a resistive antenna with a value for $R_{\rm ground}$ of 1000 Ω. This parameter is extremely difficult to measure and almost impossible to predict (Kraus & Fleisch 1999). In these field trials no special process (Petiau & Dupis 1980) was adopted to connect to the Earth as the current sink, apart from nickel coated conductors driven 20 cm into the local soil. Repeating the trials using a local electrical earth provided by power systems (and hence presumably having a much lower value of $R_{\rm ground}$) did indeed show higher levels of electromagnetic noise as expected from equation (6) but the ingress of conducted electrical noise via this earth connection could not be discounted as the cause, and these data were therefore discarded.

The conversion back from amplifier output to the ambient electric field depends on the uncertain parameter of the ground resistance. However, in comparing the detected signals with possible astrophysical source signals as in Fig. 7 the same value for $R_{\rm ground}$ was used, enabling a meaningful assessment of whether such a scheme might achieve a credible detection. Based on these very preliminary measurements a detection scheme based on a resistive antenna appears to be at least 5 or 6 orders of magnitude from detecting the brightest predicted GW events in this frequency range. While there may be avenues for reducing the ambient noise by better filtering, better control of thermoelectric effects in wiring and by improving the earthing arrangements, the electronic noise of available amplifiers and Johnson noise from the resistive wire itself are likely to limit further progress in a fundamental way.

11 CONCLUSIONS

The field trials and simulations are found to be consistent with the simple theory of the resistive antenna presented in this paper, within the available accuracy, but the tests with a controlled input have only been possible with values of $\frac{\lambda}{L}$ of 1500 and 20, respectively, much smaller than required for the frequencies planned for gravitational wave observation. It would appear from these measurements that a detection scheme based on scattering of gravitational waves from a planetary body of large magnetic moment such as the Earth would require a considerable reduction in ambient electromagnetic noise and system noise to be viable and would be limited by this ambient noise to sensitivities 6 or 7 orders of magnitude less than space-borne interferometers such as *LISA*.

ACKNOWLEDGEMENTS

The authors acknowledge support from the Science and Technology Facilities Council for part of this work and for continuing support from the University of Birmingham and University College London. This work has also been supported by a generous grant (EM 2017–100) from the Leverhulme Trust for which the authors express their gratitude. The authors wish to record their gratitude to Professor Peter Willmore with whom they had many useful discussions on this topic prior to his death in 2022 and anonymous referees who provided clarifying comments.

DATA AVAILABILITY

The data from the field trials is available on request from the authors, together with calibration curves and full description.

REFERENCES

Abbott B. P. et al., 2016, Phys. Rev. Lett., 061102, 116
Aggarwal N. et al., 2021, Living Rev. Relat., 24, 1
Boccaletti D., De Sabbata V., Fortini P., Gualdi G., 1970, Nuovo Cimento, 70, 129
Cruise A. M., 2012, Class. Quantum Gravity, 29, 0095023
De Logi W. K., Mickelson A. R., 1977, Phys. Rev. D, 16, 2915
Durand-Manterola H. J., 2009, Planet. Space Sci., 57, 1405
Gertsenshtein M. E., 1962, Sov. Phys. JETP, 14, 84
Kraus J. D., Fleisch D. A., 1999, Electromagnetics (McGraw-Hill Series in Electrical and Computer Engineering). McGraw-Hill, New York
Kraus J. D., Marhefka R. J., 2003, Antennas For All Applications. McGraw-Hill, New York
Lupanov G. A., 1967, Sov. Phys. JETP, 25, 76
Maggiore M., 2008, Gravitational Waves. Oxford Univ. Press, Oxford
Pawley E., 1972, BBC Engineering 1922–1972. BBC Publications, London, p. 445
Petiau G., Dupis A., 1980, Geophys. Prospect., 28, 792
Taflove A., Hagness S., 2005, Computational Electrodynamics 3e. Artech House Inc., Norwood, MA
V De Sabbata P. F., Gualdi C., 1974, Acta Phys. Pol., 85, 741
Vitale S., 2014, Gen. Relativ. Gravit., 46, 1730

This paper has been typeset from a TEX/LATEX file prepared by the author.